



Parametric modeling approach in laser wire additive manufacturing process

Natago Guilé Mbodj¹ · Mohammad Abuabiah^{1,2} · Maxime El Kandaoui³ · Slah Yaacoubi³ · Peter Plapper¹

Received: 26 July 2022 / Accepted: 15 December 2022 / Published online: 27 December 2022
© The Author(s) 2022

Abstract

In recent years, the evolution of computer-aided design technology has established a new design method to improve digital model creations. The new design method is called Parametric Modeling. In this paper, 3D metallic models are printed using a novel Parametric Modeling approach. The goal of this approach is to use parametric design features to simulate and print 3D metallic objects using Laser Wire Additive Manufacturing (LWAM) process. The proposed approach includes a pattern creation and robot targets assignment while considering several process requirements of LWAM and the robot system. This technique will allow the development of an adaptive robot toolpath for a good deposition process. Finally, a wall, a cylinder, and a complex shape were simulated and deposited to validate the proposed approach. The results show that the approach is feasible, adaptive, and can enhance 3D metallic print in the LWAM process.

Keywords Parametric modeling · Laser wire additive manufacturing · Adaptive toolpath · Metallic 3D printing

1 Introduction

The association between Parametric Modeling and industrial robots opens a new way to create products using

Additive Manufacturing technology (AM). Where AM is simply a 3D printer device that is usually restrained to the manufacturing of small or medium size parts [1, 2]. Nonetheless, today AM equipment can also operate to create large-scale objects as in the field of Metal Additive Manufacturing. [3, 4].

Metal Additive Manufacturing process began in the late 1990s [5, 6]. According to different sources of energy used for metal deposition, Metal Additive Manufacturing could be classified into Arc Additive Manufacturing, Electron Beam Additive Manufacturing, and Laser Additive Manufacturing [7]. With regard to the additive material form, Laser Additive Manufacturing could be divided into powder-based and wire-based Laser Additive Manufacturing. In this study, we will focus on the Laser Wire Additive Manufacturing (LWAM) technology.

The process of LWAM consists of melting a wire using an energy source to create a liquid melt pool bead. The beads are then added layer by layer to form the final object, as shown in Fig. 1. Today's application of the process can be found in the automotive sector, aircraft, medical implants, dental restoration, and even the fashion sector [8–10].

Despite the advances in AM, there are still many challenges related to the process applicability, cost, and deposition process parameters [5, 8, 10–13]. However, one of the main challenges in AM, especially in LWAM, is the understanding and knowledge of the combination of

This article belongs to the Topical Collection: *Additive Manufacturing Processes and Performance*

✉ Natago Guilé Mbodj
natago.mbodj@uni.lu

✉ Mohammad Abuabiah
mohammad.abuabiah@uni.lu

Maxime El Kandaoui
m.elkandaoui@isgroupe.com

Slah Yaacoubi
s.yaacoubi@isgroupe.com

Peter Plapper
peter.plapper@uni.lu

¹ Department of Engineering, University of Luxembourg, 6, rue-Kalergi, Luxembourg, L-1359, Luxembourg

² Department of Mechanical and Mechatronics Engineering, An-Najah National University, P.O. Box 7, Nablus, Palestine

³ Plateforme DRIEG CND and Assembly, Institut de Soudure, 4 Bd Henri Becquerel, Yutz, 57970, France

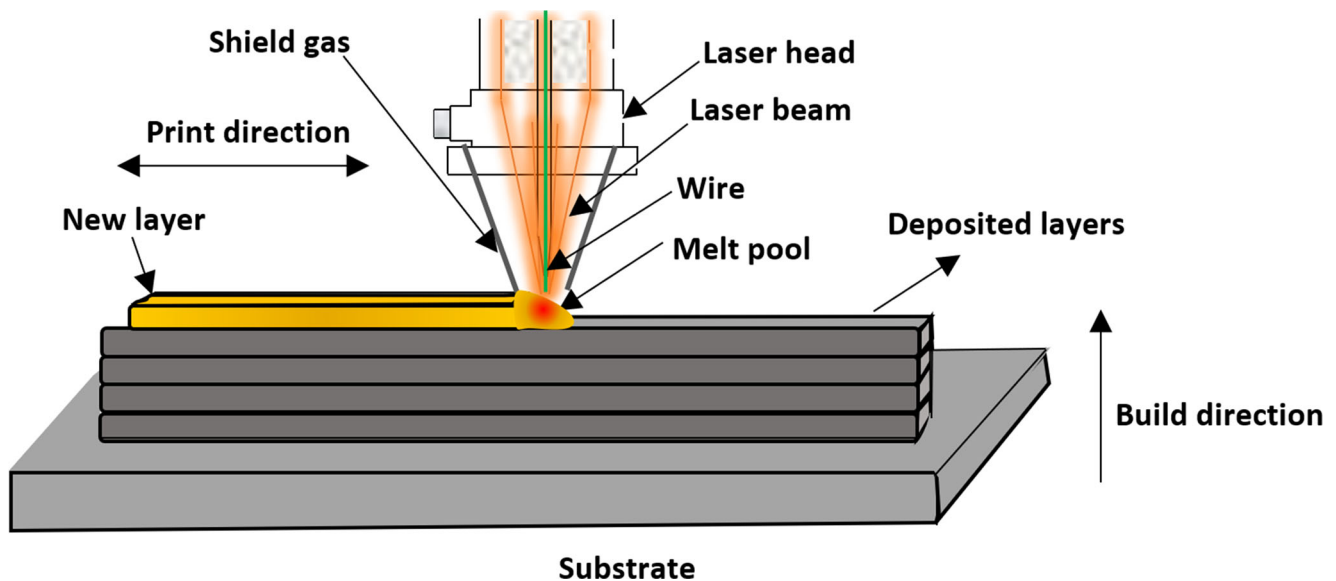


Fig. 1 Schematic diagram of Metal Additive Manufacturing

the system's software and hardware. On the other hand, standard G-code is usually employed by 3D technology to print the final parts. 3D printers use only linear commands of the G-code to define the printing paths, whether the motions are linear or circular. Consequently, the G-code becomes complex for curves creation as the curve is approximated using many straight lines [14]. Thus, one problem with the G-code technique is that it can be inadequate to create complex parts [15]. Furthermore, it is complicated to convert a G-code to a 3D deposition path, for complex objects, that are usable by the robot [16]. These extra works frequently result in simulation errors, time loss and process errors [17].

To overcome such limitations, a method called Parametric Modeling (PM) is developed to 3D print using a robot for large-scale manufacturing processes and complex objects [18]. The evolution of computer-aided design technology imposes the creation of this method to improve the digital model creations. PM method helps the development of 3D printing in the industry to create parts on large scales using an automatic layer-by-layer deposition process [16].

Few studies can be reported using parametric designs in 3D printing technology. In [18, 19], Kontovourkis et al. presented two works related to developing a parametric design algorithm and an automated system for additive manufacturing for 3D clay printing. In [18], the authors gave an insight for 3D clay printing using a parametric environment and a robot. While in [19], Kontovourkis et al. showed the development of a parametric-integrated algorithm for 3D printed earth and clay-based materials using an industrial robot. On the other hand, Fischer et al. [20] presented an overview of concrete 3D printing and an online parametric customization and fabrication of small 3D

concrete printed pavilions. While Jeong et al. [21], used a parametric design method to create 3D printed wearable fashion products using the Fused Deposition Modeling (FDM) process. The work demonstrated that parametric design method features could produce fashion products. In [22], Naddeo et al. used parametric algorithms in a finite element environment to simulate curved beam lattice structure. The comparison between the numerical results and experimental results confirmed the validity of this approach that could be used for different solid shapes. Finally, Lim et al. [16] proposes a parametric design to generate curved-layered printing paths for large-scale construction processes. Scripting languages are used to slice layers and provide printing paths adjustable interactively to fit various shapes. The paths are converted to G-Code and extra CNC-related commands such as the nozzle on/off and pump start/stop commands, speed control of the pump, etc. added later.

Based on the brief introduction, and to the best author's knowledge, the Parametric Modeling approach has not been yet developed and adapted to the LWAM technology. Therefore, this work aims to print 3D metallic models using a novel parametric modeling design framework in the LWAM process. More specifically, the proposed parametric model includes the main process parameters (power, wire-feed rate, travel speed, bead geometry), skips the G-Code conversion step and provides directly a 3D printing code for the assigned robot (see Fig. 2). The proposed approach also offers a user-friendly method for printing metal objects and taking into consideration different process requirements. For the validation, a wall, a hollow cylinder and a complex shape model will be simulated and experimentally printed to confirm the feasibility of the proposed approach. The paper

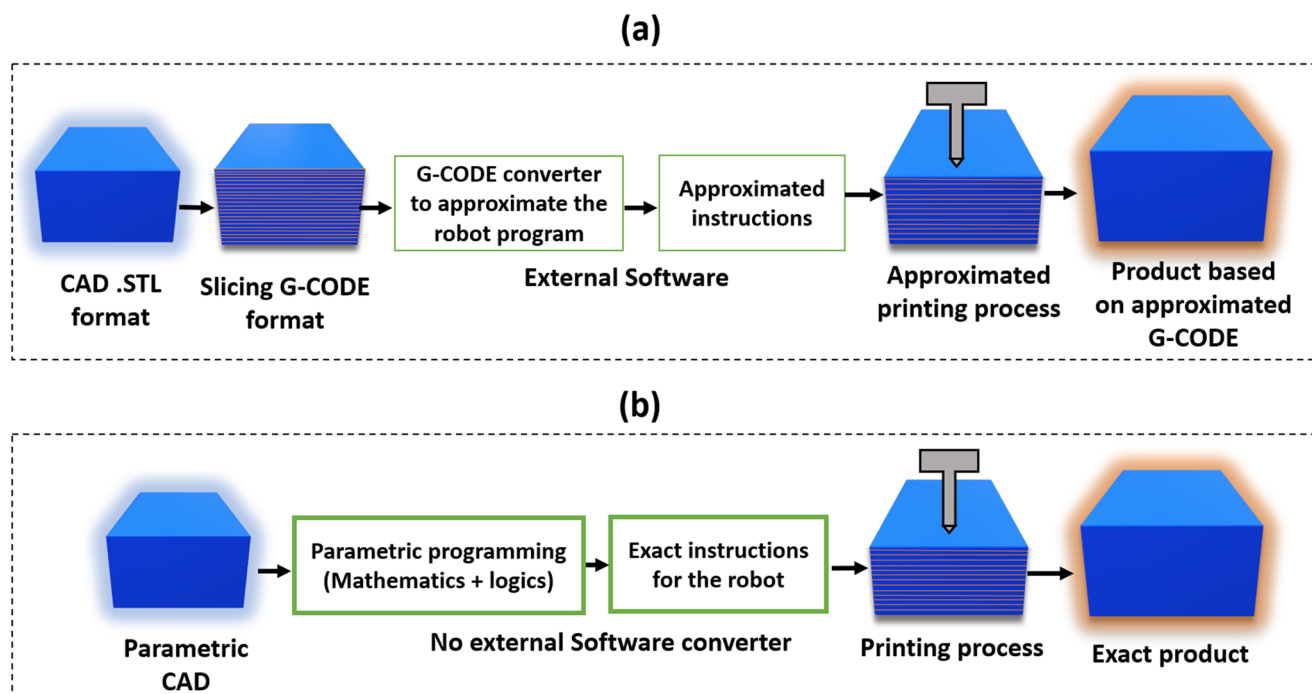


Fig. 2 (a) Conventional 3D printing using G-code approach; (b) proposed 3D printing technique using Parametric Modeling Approach

is structured as follows, Section 2 introduces methodology, while Section 3 presents the experimental results and discussion. The paper finishes in Section 4 with conclusion and remarks.

2 Methodology

The association between Parametric Modeling and industrial robots opens a new way to create products. This association needs an understanding and knowledge of the system’s software and hardware. In this section, a methodological frame that integrates a parametric implementation for large-scale manufacturing parametric design using an industrial robot system to 3D print metallic parts is developed. More specifically, this work provides a sustainable and open-source framework to print medium and large sizes parts in a single adaptive environment. The work considers the LWAM process as a case-of-study including all its process parameters and bead geometry. Also, it includes a descriptive workflow from the CAD part to the manufacturing part.

In LWAM process, the process parameters play an important role in the final product. The process parameters choice such as the laser power, the wire feed rate and the travel speed have an influence on the robot toolpath planning. The toolpath planning includes contour creation, layer height (adaptive or fixed thickness), printing direction, path pattern, and bead geometry settings. Therefore, process

planning is important to create a homogeneous and stable printing process. In this work, Grasshopper software is employed to achieve the task. Where, Grasshopper is a visual programming language (VPL) developed in 2007 by McNeel Corporation [23].

Both, parametric and non-parametric CAD models can be created or imported within Grasshopper software. In this work, both approaches will be performed for toolpath creation. The proposed method enables to produce digitally various shapes and design possibilities parametrically, as shown in the flowchart illustrated in Fig. 3. The parametric design creation is embedded in the bead width and height, layer heights, contour, and toolpath. Then, a robotic control plug-in for Rhino called HAL software [24] is used to convert each defined point to robot targets. Finally, a robot programming language is used to include printing process parameters and data related to the robot system to produce the deposition executable by the robotic arm.

Figure 3 shows that the proposed parametric 3D printing process begins with first creating a parametric surface. In this step, a cross-section of the CAD model is created. Mathematical formulas of regular shapes (square, rectangle, triangle, circle, parallelogram, etc.) are used to create the cross-section of the final object. The object dimension and its cross-sectional area parameters are given as predefined inputs, as illustrated in Fig. 4.

After the 2D surface is created, patterns are added to it. In most 3D printing processes, patterns such as raster, zigzag, contour, or concentric are commonly used in AM

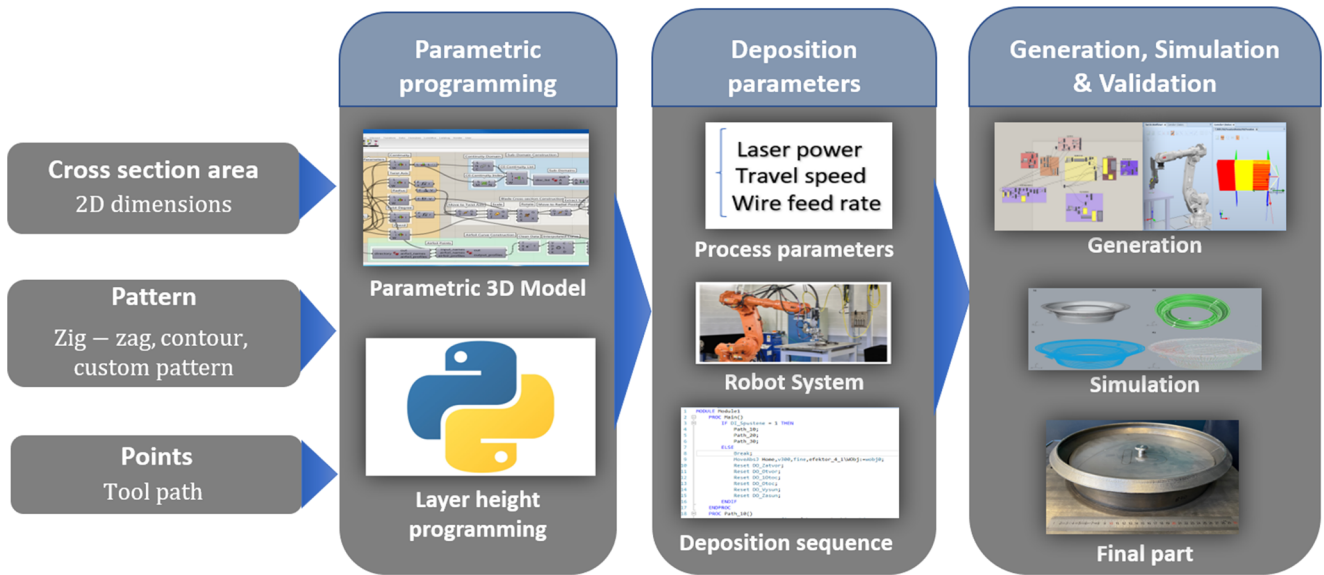


Fig. 3 Parametric 3D printing flowchart for the LWAM process

(see, e.g., [25]). The patterns are created based on the bead geometry dimension, mainly the bead width dimension. The step-by-step process of pattern creation is shown in Fig. 5 and Fig. 6.

The next step is to assign points to the generated patterns. These points will later be used by the robot as targets. The points are arranged and connected sequentially to form the toolpath pattern for the robot, as shown in Fig. 7. Noting that, after placing the points on the first layer, the generated toolpath is then copied to the other layers with fixed or variable thicknesses using a Python script. A layer thickness algorithm (see, e.g., [13]) is run in the script to create the toolpath patterns for each layer.

Hereafter, a layer-to-layer travel strategy is implemented. The travel strategy is created by selecting and connecting the last point of each layer to the first point of the next layer, or vice-versa. Defining a suitable travel strategy is crucial and affects the final object geometry in terms of cooling and the bonding between layers. Lastly, all created points will be converted to robot targets to generate the 3D printing program. HAL framework is used to convert the

created points to robot targets. Finally, a digital parametric object, convertible into many robot programs, is now created and ready to be used by the industrial robot to perform the printing process.

Remark 1 HAL is a Grasshopper plug-in allowing the translation of parametric designs to industrial robot programs. After the robot targets are created, deposition process parameters (power, wire feed rate, travel speed), the robot system (tool frame, object frames, task frames) and the deposition sequences (wait time, stop, etc) are added to the final program.

3 Results verification

In this section, three cases of study (wall, hollow cylinder, and complex model) will be simulated and printed to validate the proposed approach. The printing process starts at an assigned point in the object where deposition process parameters are activated simultaneously. The toolpath is

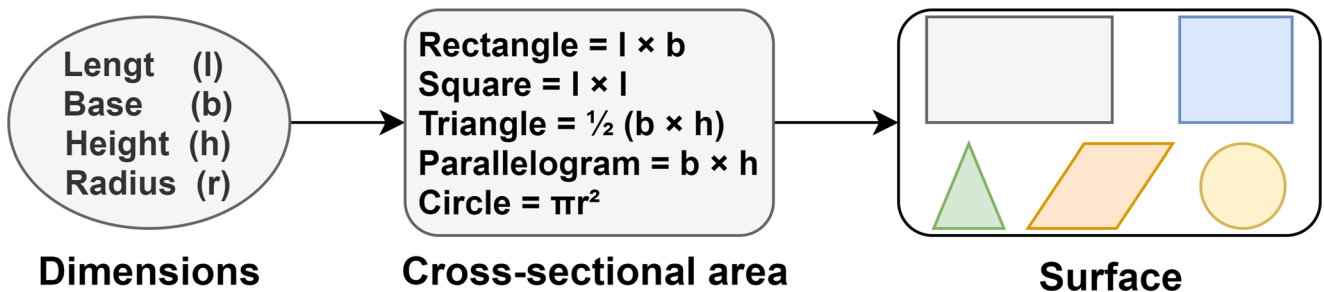


Fig. 4 Cross section creation

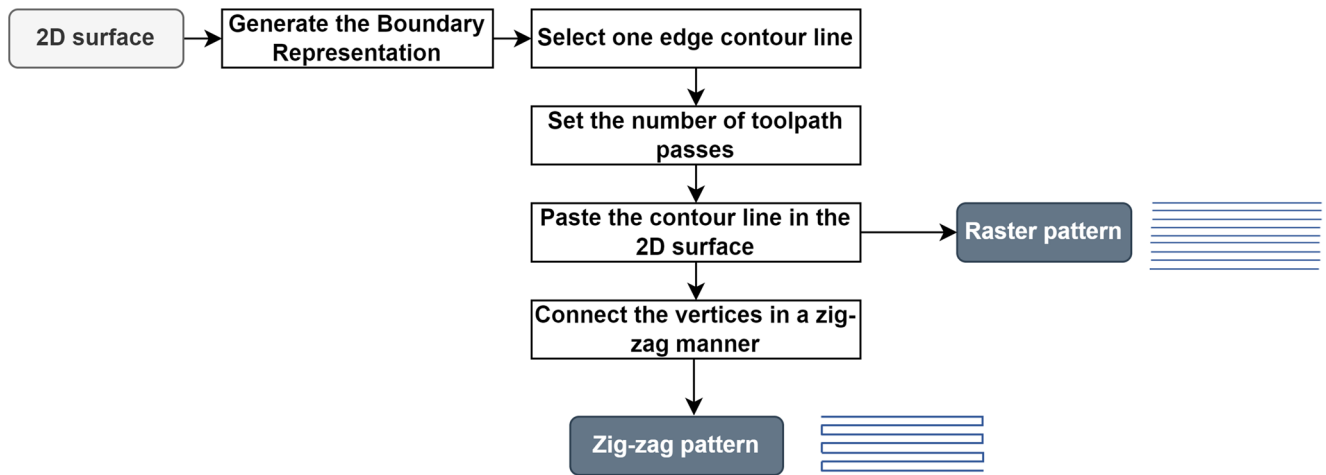


Fig. 5 Pattern creation for raster and zig-zag patterns

reproduced layer by layer until the full part is created and the final object is completely simulated. After completion, the program is transferred to RobotStudio where the deposition sequences are added based on the deposition requirement. The full program is then sent to the robot controller to execute the printing process. The real robot follows the virtual simulation following the robot targets where frames are assigned to each of them. If a problem occurs, meaning the programmed points do not coincide with the real points, stop instructions integrated at specific points of the program will stop the deposition process. This will ensure

that the final part is printed correctly without collision or undesirable movements that may occur.

Experimental test for the three cases studies were carried out on the laser platform at Institut de Soudure. Tests were run by a robotized laser wire-feed system. An ABB 7-axis poly-articulated robot was used to provide the kinematics of the process. A fibre laser source, IPG Photonics, of 10 kW was used as the heat source. The system also used a CoaxPrinter laser processing head to deliver the laser beam and the filler wire to the processing zone. Figure 8 shows the actual LWAM system setup.

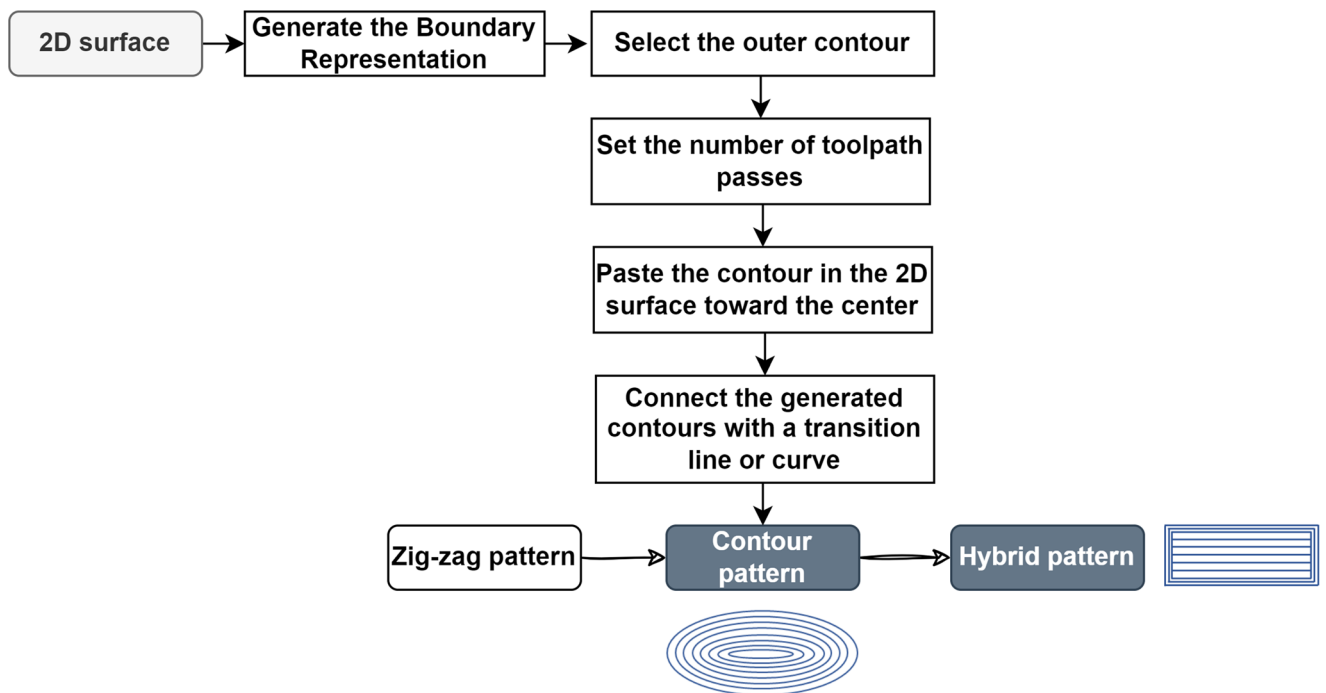


Fig. 6 Pattern creation for contour and hybrid patterns

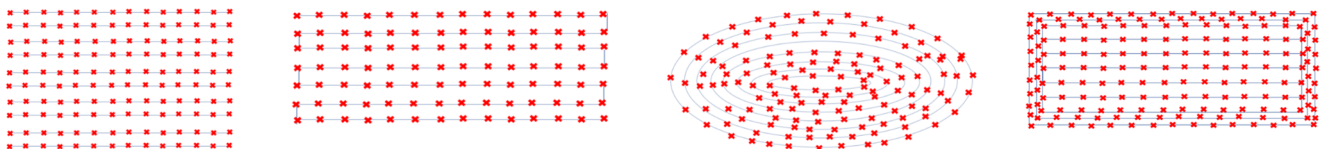
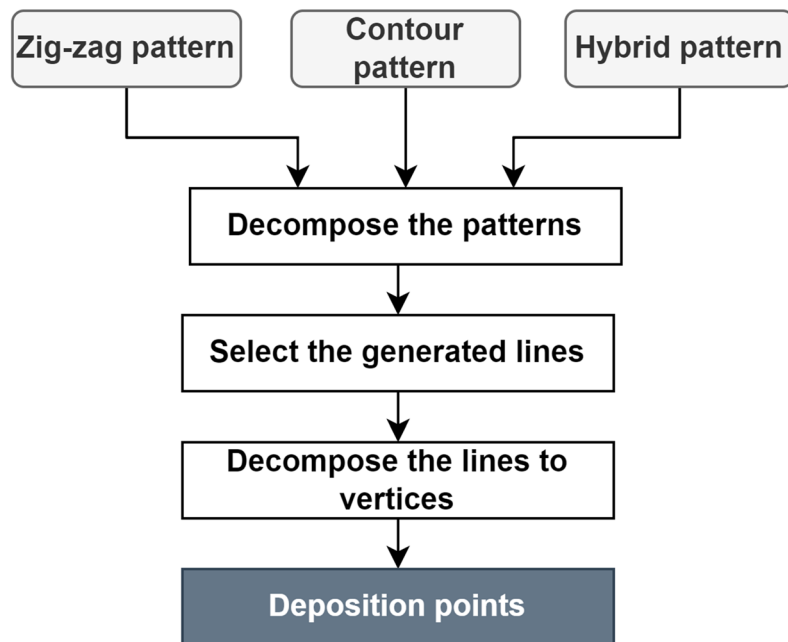


Fig. 7 Points creation for zig-zag, contour, and hybrid patterns

3.1 Case 1: Wall

The first test, to validate the proposed approach, is to simulate and print a metal wall object using the LWAM technique. The construction steps for the wall printing are divided into the following steps: (i) defining the wall's dimension (length and width). (ii) Pattern creation using the approach discussed in Section 2. In this step, the distance between passes (filling density) is chosen according to the

bead geometry dimension. (iii) Defining the layer height thicknesses and the layer by layer travel strategy. (iv) Assigning points to the defined pattern and converting them as robot targets. (v) Defining the robot program parameters, such as the robot frames (tool, task, object), the process parameters (see Table 1) and the deposition sequences (stop time, wait time, process parameters ON and OFF sequences). (vi) Finally, the wall object is simulated and the program is transferred to the robot controller for

Fig. 8 Experimental setup of LWAM platform at Institut de Soudure

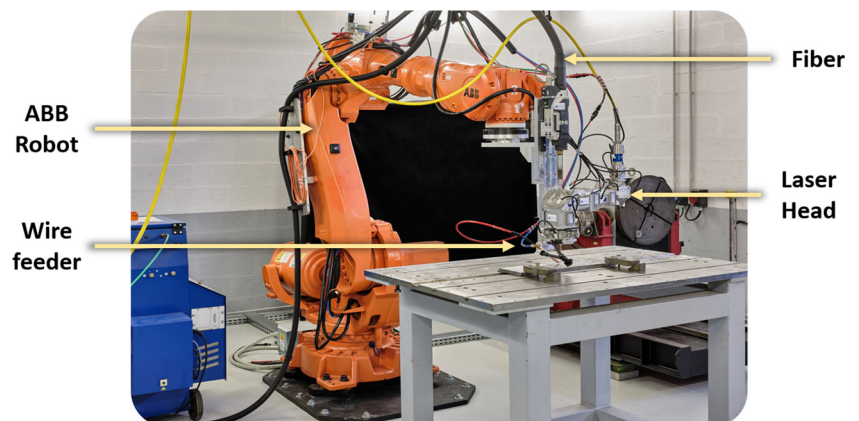


Table 1 Case 1: Wall deposition parameters

Power (W)	Travel speed (m/min)	Wire-feed rate (m/min)	Number of passes	Number of layers
2200	1.2	1.8	10	61

the experimental deposition process. Figure 9 shows the result of the wall creation. From the result, we can notice the flexibility of the proposed technique to print a metal wall object without the need for the G-code and having similar printing object output compared with the simulation result.

3.2 Case 2: Hollow cylinder

The second test, to validate the proposed approach, is to simulate and print a metal hollow cylinder object using the LWAM technique. The construction steps for the hollow cylinder printing are similar to those discussed in Case 1. For this case, a contour toolpath is designed, and the deposition parameters are given in Table 2. The result in Fig. 10 shows a printed hollow cylinder object that is similar to the simulated output using the proposed approach and without the need for the G-Code.

3.3 Case 3: Complex model

The final test is to simulate and print a complex metal object using the LWAM to validate the proposed approach. For any complex objects that are difficult to create parametrically,

Grasshopper offers tools to automatically parametrize such an object. The modified process steps for printing such a complex object are the following (see also Fig. 11): (i) the CAD file for the required model is imported into the parametric programming framework. (ii) Then, the CAD model is converted to a parametric CAD file. (iii) A BREP method is used to create a boundary representation of the CAD model, where the boundary representation is composed of the boundary of the model, the solids, the vertices, the edges and the faces, as illustrated in Fig. 12. (iv) The parametrized CAD is used then to define the layers, the pattern, the points and the converted robot targets, as it was discussed in the previous section.

The deposition parameters for printing the complex model using LWAM are summarized in Table 3. Furthermore, Fig. 13 shows the final results of the printed model using the proposed Parametric Modeling approach. The result shows a good match between the given 3D model of a complex object and the final metal product.

The dimensional of the printed products and the 3D model objects for the three cases are compared in Table 4. This table shows good agreement between the dimension of the printed metal product and the assigned 3D model with relatively small errors.

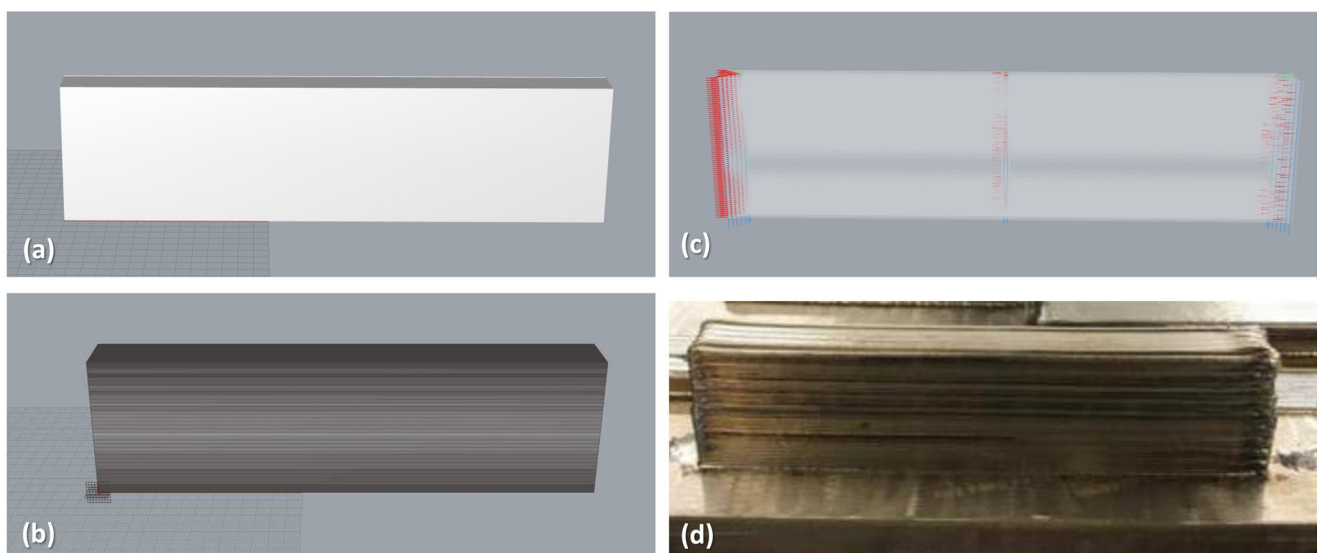


Fig. 9 Case 1 (a) wall 3D model object, (b) wall pattern creation, (c) wall points creation, (d) printed metal wall output

Table 2 Case 2: Hollow cylinder deposition parameters

Power (W)	Travel speed (m/min)	Wire-feed rate (m/min)	Number of passes	Number of layers
2200	1.2	1.8	2	130

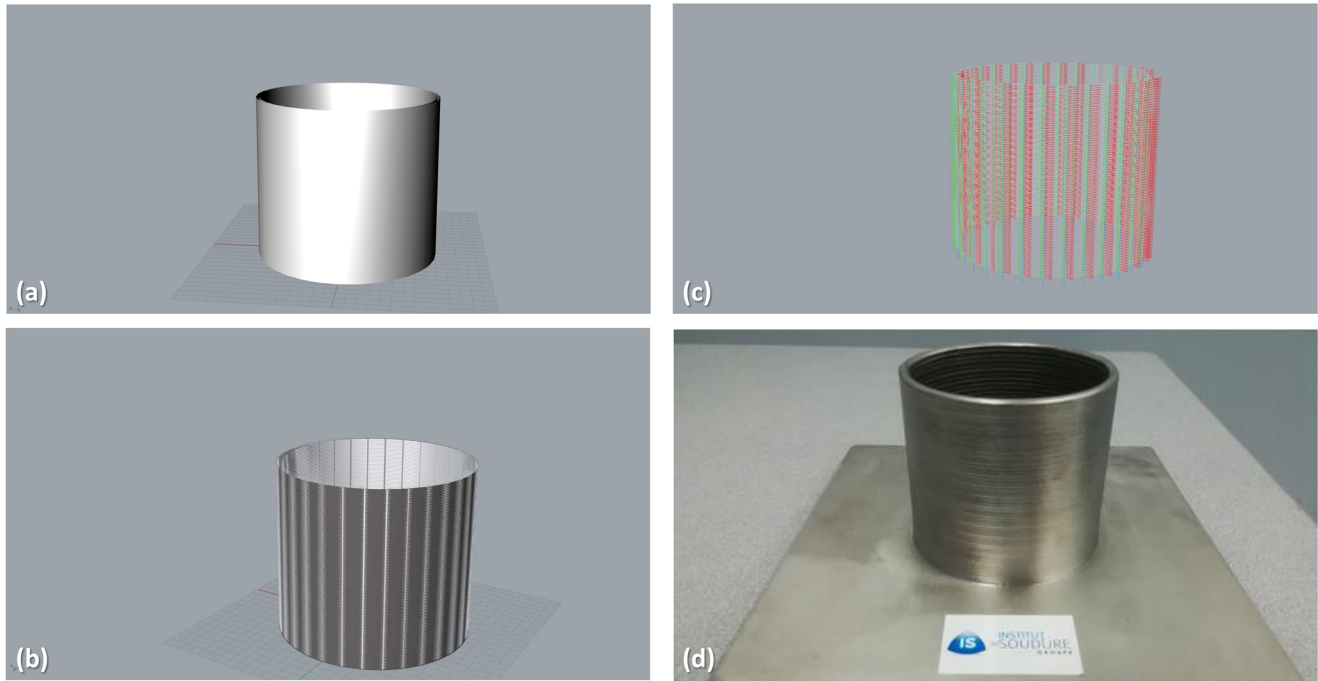


Fig. 10 Case 2 (a) hollow cylinder 3D model object, (b) hollow cylinder pattern creation, (c) hollow cylinder points creation, and (d) printed metal hollow cylinder output

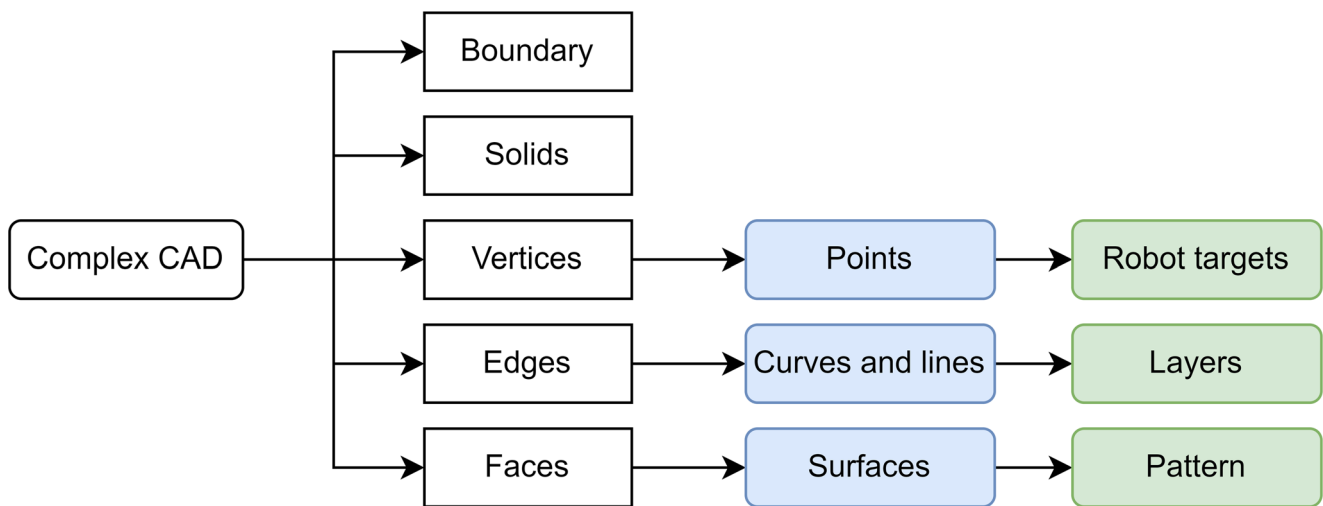


Fig. 11 Parametrization flowchart for complex objects

Fig. 12 Parametrization of the proposed CAD model (the 3D model is provide by SAFRAN Aircraft Engine under FAFil INTERREG project)

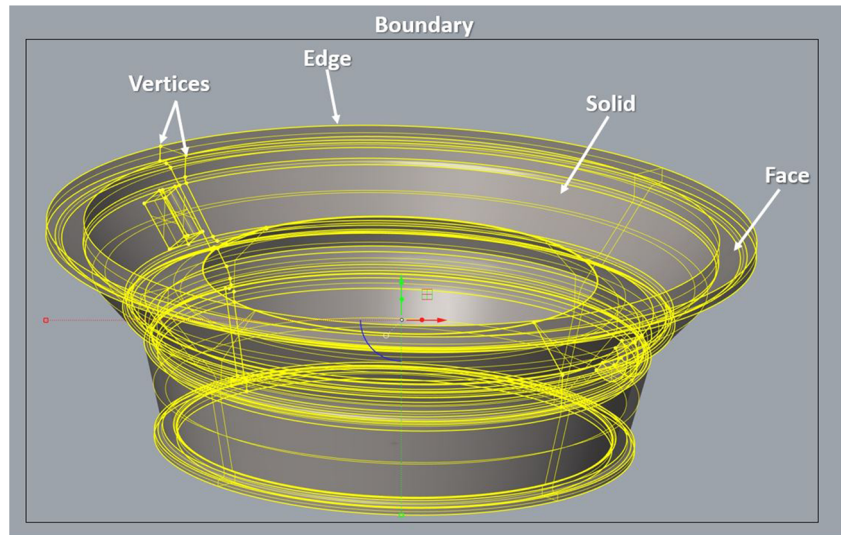


Table 3 Case 3: Complex model deposition parameters

Power (W)	Travel speed (m/min)	Wire-feed rate (m/min)	Number of passes	Number of layers
2700	2.0	2.2	2	56

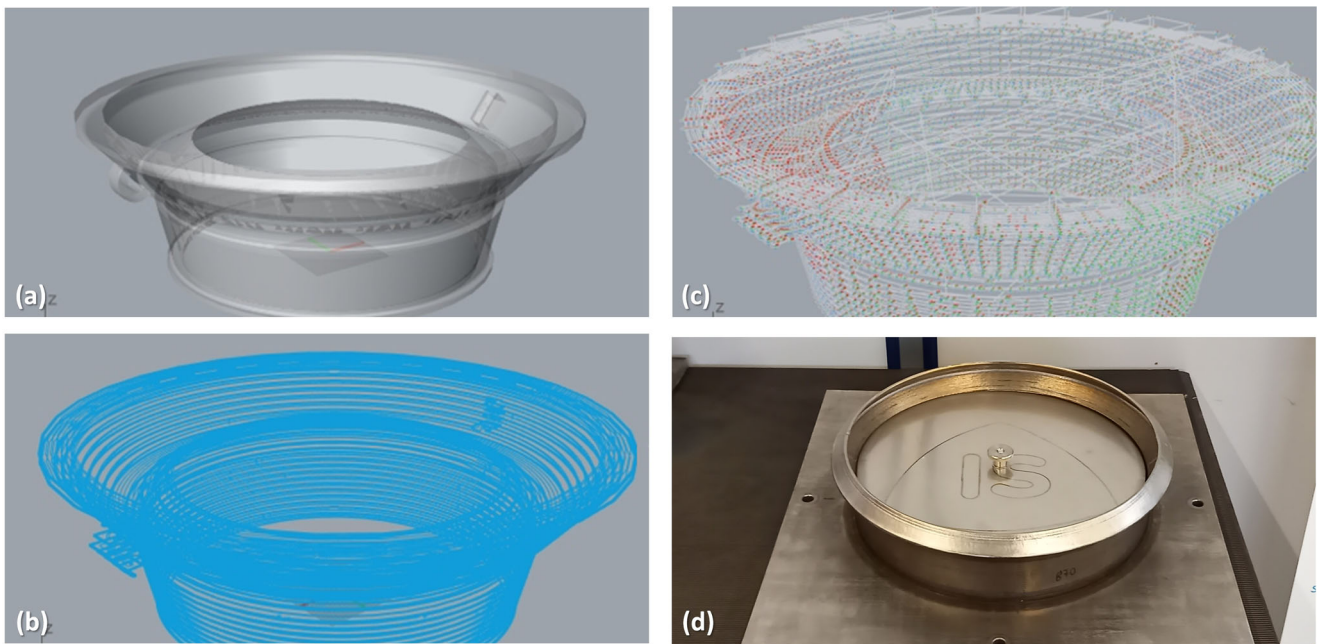


Fig. 13 Case 3 (a) complex 3D model object, (b) complex model pattern creation, (c) complex model points creation, (d) printed metal complex object output

Table 4 Comparison of the dimension between the printed product and 3D model for the three cases

Cases	3D model	Printed product	Relative percentage error
Case 1: Wall	190 × 50 × 20 mm (L × W × H)	184 × 49 × 18 mm	3.58%
Case 2: Cylinder	100 × 80 mm (D×H)	91 × 80 mm	5.00%
Case 3: Complex model	100 and 5 mm (H×W)	94 and 4 mm	7.15%

4 Conclusion

In this paper, a novel Parametric Modeling approach was developed for the LWAM process. The goal of the proposed approach was to use parametric design features to simulate 3D deposition paths for printing large scale metals using LWAM technology. The proposed approach includes a pattern creation and robot targets assignment while considering several deposition parameters and process requirements.

The experimental results revealed that the developed Parametric Modeling approach is capable of printing large scales metals using an automatic layer-by-layer deposition process without the need for using G-code. The results were conducted using three different cases namely, a wall, a hollow cylinder and a complex model. For each case, the results show that the approach is feasible, adaptive, and is able to print precise 3D metallic objects using the LWAM process.

Acknowledgements The authors would like to thank the Institut de Soudure—Yutz, for providing the experimental data. Also, the authors would like to thank SAFRAN Aircraft Engine for providing the complex 3D model.

Author contribution Conceptualization, methodology, investigation, and original draft preparation: N.G.M. and M.A.; review and editing: N.G.M., M.A., P.P., M.E.K., and S.Y.; supervision: P.P.; project administration and funding acquisition: P.P. and M.E.K.

Funding This research was funded by the Interreg V-A Grande Région “Fabrication Additive par Dépôt de Fil” (FAFil) project (Ref. 3477).

Declarations

Consent to participate All authors agree to take part in this study.

Consent for publication All authors have read and agreed to the published version of the manuscript.

Conflict of interest The authors declare no competing interests.

Open Access This article is licensed under a Creative Commons Attribution 4.0 International License, which permits use, sharing, adaptation, distribution and reproduction in any medium or format, as long as you give appropriate credit to the original author(s) and the source, provide a link to the Creative Commons licence, and indicate if changes were made. The images or other third party material in this article are included in the article’s Creative Commons licence, unless indicated otherwise in a credit line to the material. If material is not included in the article’s Creative Commons licence and your intended use is not permitted by statutory regulation or exceeds the permitted use, you will need to obtain permission directly from the copyright holder. To view a copy of this licence, visit <http://creativecommons.org/licenses/by/4.0/>.

References

- Chang H-C (2021) Parametric design used in the creation of 3D models with weaving characteristics. *J Comput Commun* 09:112–127. <https://doi.org/10.4236/jcc.2021.911008>
- Bai X, Huerta O, Unver E, Allen J, Clayton JE (2021) A parametric product design framework for the development of mass customized head/face (eyewear) products. *Appl Sci* 11:5382. <https://doi.org/10.3390/app11125382>
- Khorasani AM, Gibson I, Goldberg M, Littlefair G (2016) A survey on mechanisms and critical parameters on solidification of selective laser melting during fabrication of ti-6al-4v prosthetic acetabular cup. *Mater Des* 103:348–355. <https://doi.org/10.1016/j.matdes.2016.04.074>
- Sreekanth S, Ghassemali E, Hurtig K, Joshi S, Andersson J (2020) Effect of direct energy deposition process parameters on single-track deposits of alloy 718. *Metals* 10:96. <https://doi.org/10.3390/met10010096>
- Sing SL, Tey CF, Tan JHK, Huang S, Yeong WY (2020) 3D printing of metals in rapid prototyping of biomaterials: techniques in additive manufacturing. *Rapid Prototyping of Biomaterials*, 17–40. <https://doi.org/10.1016/B978-0-08-102663-2.00002-2>
- Molitch-Hou M (2018) Overview of additive manufacturing process
- Huang W, Chen S, Xiao J, Jiang X, Jia Y (2021) Laser wire-feed metal additive manufacturing of the al alloy. *Optics & Laser Technol* 134:106627
- Yakout M, Elbestawi MA, Veldhuis SC (2018) A review of metal additive manufacturing technologies. *Solid State Phenom* 278:1–14. <https://doi.org/10.4028/www.scientific.net/SSP.278.1>
- Saboori A, Aversa A, Marchese G, Biamino S, Lombardi M, Fino P (2019) Application of directed energy deposition-based additive manufacturing in repair. *Appl Sci* 9:3316. <https://doi.org/10.3390/app9163316>
- Domack CS (2020) T.K.M.: Challenges in metal additive manufacturing for large-scale aerospace applications, in women in aerospace materials. Springer, Cham, pp 105–124
- Zenou M, Grainger L (2018) Additive manufacturing of metallic materials. *Additive Manufacturing*, 53–103. <https://doi.org/10.1016/B978-0-12-812155-9.00003-7>
- Donadello S, Motta M, Demir AG, Previtali B (2019) Monitoring of laser metal deposition height by means of coaxial laser triangulation. *Opt Lasers Eng* 112:136–144. <https://doi.org/10.1016/j.optlaseng.2018.09.012>
- Mbodj NG, Abuabiah M, Plapper P, Kandaoui ME, Yaacoubi S (2021) Bead geometry prediction in laser-wire additive manufacturing process using machine learning: Case of study. *Appl Sci* 11:11949. <https://doi.org/10.3390/app112411949>
- Pan Y. (2021) Simplify robot programming with g-code. <https://www.universal-robots.com/blog/simplify-robot-programming-with-g-code>. Accessed: 27-12-2021
- Hu B, Jin G, Sun L (2018) A novel adaptive slicing method for additive manufacturing. In: 2018 IEEE 22nd International Conference on Computer Supported Cooperative Work in Design ((CSCWD)), pp 218–223. <https://doi.org/10.1109/CSCWD.2018.8465247>
- Lim S, Buswell RA, Valentine PJ, Piker D, Austin SA, Kestelier XD (2016) Modelling curved-layered printing paths for fabricating large-scale construction components. *Additive Manuf* 12:216–230. <https://doi.org/10.1016/j.addma.2016.06.004>
- Nilsson D. (2016) G-Code to RAPID translator for Robot-Studio
- Kontovourkis O, Tryfonos G (2018) Integrating parametric design with robotic additive manufacturing for 3D clay printing: an experimental study. <https://doi.org/10.22260/ISARC2018/0128>

19. Kontovourkis O, Tryfonos G (2020) Robotic 3D clay printing of prefabricated non-conventional wall components based on a parametric-integrated design. *Autom Constr* 110:103005. <https://doi.org/10.1016/j.autcon.2019.103005>
20. Fischer T, Herr C (2016) Parametric customisation of a 3D concrete printed pavilion
21. Jeong J, Park H, Lee Y, Kang J, Chun J (2021) Developing parametric design fashion products using 3D printing technology. *Fashion and Textiles* 8:22. <https://doi.org/10.1186/s40691-021-00247-8>
22. Naddeo F, Naddeo A, Cappetti N (2017) Novel “load adaptive algorithm based” procedure for 3D printing of lattice-based components showing parametric curved micro-beams. *Compos Part B: Eng* 115:51–59. <https://doi.org/10.1016/j.compositesb.2016.10.037>
23. Nagy D. (2020) Computational design in Grasshopper. <https://medium.com/generative-design/computational-design-in-grasshopper-1a0b62963690>. Accessed: 05-2020
24. Schwartz T (2013) Hal: Extension of a visual programming language to support teaching and research on robotics applied to construction. *Rob Arch* 2012. Springer, Vienna, pp 92–101
25. Ding D, Pan ZS, Cuiuri D, Li H (2014) A tool-path generation strategy for wire and arc additive manufacturing. *Int J Adv Manuf Technol* 73(1):173–183

Publisher’s note Springer Nature remains neutral with regard to jurisdictional claims in published maps and institutional affiliations.